www.czasopisma.pan.pl PAN POLSKA AKADEMIA NAUK www.journals.pan.pl

A R C H I V E S O F M E T A L L U R G Y A N D M A T E R I A L S

Volume 60 2015 Issue 4

DOI: 10.1515/amm-2015-0404

CAO XIAOZHOU*,#, WANG CHAO*, XUE XIANGXIN*, CHENG GONGJIN*

EFFECT OF TI ADDITION ON THE RESIDUAL ALUMINIUM CONTENT AND MECHANICAL PROPERTIES OF THE B_4C-Al COMPOSITES PRODUCED BY VACUUM INFILTRATION

WPŁYW DODATKU TYTANU NA RESZTKOWĄ ZAWARTOŚĆ ALUMINIUM I WŁAŚCIWOŚCI MECHANICZNE KOMPOZYTÓW B_4C-Al WYTWORZONYCH PRZEZ INFILTRACJĘ PRÓŻNIOWĄ

The effect of Ti addition on the residual Al content and mechanical properties of B_4C-Al composites fabricated by vacuum infiltration was investigated in the present study. The B_4C-Al composite materials were fabricated using [Ti+B_4C] preforms preheated at 1700ºC for 1 h and Al alloys infiltrated in vacuum atmosphere at 1100ºC for 2 h. The phase composition indicated that TiB_2 has high wettability to Al as a result of the preheating. SEM and EDX results revealed a number of Al dimples are on the fracture surface due to the existence of TiB_2. When the content of added Ti increases to 30%, the [Ti+B_4C] preform is characterized by a minimal porosity (33.11%) and a maximal density, a corresponding amount of residual Al of 33.11% and a minimal fracture toughness (5.03 MPa·$m^{1/2}$) with a hardness of up to 63 HRC. The residual Al and the mechanical properties of the composite material preform were determined by the Ti content of the preform.

Keywords: Ti; B_4C; residual Al; infiltration; interface reaction

Zbadano wpływ dodatku tytanu na resztkową zawartość Al i właściwości mechaniczne kompozytów B_4C-Al wytworzonych przez infiltrację próżniową. Kompozyty B_4C-Alzostały wytworzone przez infiltrację stopów Al, w próżni, w 1100ºC przez 2 godziny, do wstępnie wygrzanych w 1700ºC przez 1 godzinę preform [Ti+B_4C]. Faza TiB_2 charakteryzuje się wysoką zwilżalnością przez Al na skutek wstępnego wygrzania. Wyniki analizy SEM i EDX ujawniły pewną liczbę wgłębień Al znajdujących się na powierzchni pęknięcia z uwagi na obecność TiB_2. Gdy zawartość dodanego Ti wzrasta do 30%, preforma [Ti+B_4C] charakteryzuje się minimalną porowatością (33,11%) i maksymalną gęstością, odpowiednią ilością resztkowego Al tj. 33.11%, minimalną odpornością na kruche pękanie (5,03 MPa·$m^{1/2}$), i twardością do 63 HRC. Resztkowe Al i właściwości mechaniczne materiału kompozytowego preformy determinowane są przez zawartość Ti w preformie.

1. Introduction

Boron carbide (B_4C) ceramics have excellent physical and mechanical properties, such as a high melting point and hardness, good abrasion resistance, high impact resistance, excellent resistance to chemical agents and high neutron absorption capabilities[1-6]. As a good ceramic material, boron carbide (B_4C) has attracted attention in a wide variety of applications, including light-weight armour plating, blasting nozzles, mechanical seal faces, grinding tools, cutting tools and neutron absorption materials. However, B_4C ceramics are hardly sinterable and relatively brittle and thus face serious obstacles for any structural material because of their low flexural strength (200–300 MPa) and fracture toughness (2–3 MPa·$m^{1/2}$)[3, 7-9].

Recently, Al/B_4C composites have received attention because they feature the mechanical properties of B_4C enhanced by Al infiltration to the ceramic material[10, 11]. However, a large amount of reaction products are formed during the infiltration process at high temperatures. It has been reported that approximately 30 vol.% of new phases occur from initially 38 vol.% aluminium and 62 vol.% B_4C[11-13]. The reaction products tend to form large, granular clusters, resulting in a lower strength regardless of the phase. Meanwhile, the toughness is also considerably reduced.

Lee et al. prepared TiB_2-coated B_4C powder using B_4C powder and $Ti(OH)_4$ via the sol–gel process. The new generation of TiB_2 has reasonable wettability with aluminium, which can greatly enhance infiltration kinetics during the preparation of B_4C/Al composite[11].

Du et al. found that AlB_{12} addition can improve the mechanical properties of B_4C-Al, which is attributed to the existence of a metastable stress-induced phase transition of AlB_{12} from the β-phase to the α-phase below 1550°C[14]. However, the infiltration temperature was too high to reduce the interface reaction.

Lü et al. reported that TiB_2 synthesized in situ from B_4C and TiO_2 could effectively improve the mechanical properties of

* SCHOOL OF MATERIALS AND METALLURGY, NORTHEASTERN UNIVERSITY, SHENYANG 110819, CHINA

** Corresponding author: caoxz@smm.neu.edu.cn

the B_4C–TiB_2–Al composite fabricated by vacuum infiltration with B_4C and Al[15]. However, extraneous elements entered the composite, leading to the presence of more impurities in the composite materials.

The effect of Ti addition on preform porosity in the preheated process has not been studied. In addition, no studies have reported the effect of Ti addition on the residual amount of Al and the corresponding mechanical properties of B_4C-Al affected by the preform porosity.

In the present study, high-volume-fraction B_4C-Al composite materials including four different preform Ti contents were fabricated by the vacuum infiltration method. The effect of Ti addition on the preform porosity, residual amount of Al and corresponding mechanical properties of the B_4C-Al composites were discussed. To reduce oxygen disturbance, the infiltration process was performed under vacuum.

2. Experimental

The starting materials used in this work were Ti powder (99.8% purity, average particle size under 38 μm), B_4C powder (97% purity, average particle size under 15 μm) and aluminium alloy (trademark 5083). The chemical composition of the aluminium alloy is shown in Table 1.

The Ti and B_4C powders were blended using a rolling ball mill with polyurethane balls for 24 h. Next, the Ti-B_4C powder was mixed with PF resin-acetone solution as an adhesive. The resulting powders were granulated using a 60-mesh sieve for further use, and the mixtures were uniaxially cold pressed into 30-mm-diameter preforms in a stainless-steel die under 150 MPa maintained for 1 min.

TABLE 1
Chemical composition of the aluminium alloy (trademark 5083 wt.%)

Alloy	Al	Si	Cu	Mg	Zn	Mn	Ti	Cr	Fe
wt.%	93.15-94.55	0.4	0.1	4.0-4.9	0.25	0.1-0.4	0.15	0.05-0.25	0.4

2.1. Composite Preparation

[Ti+B_4C] preforms with different Ti contents (S1: 10% Ti; S2: 20% Ti; S3: 30% Ti; S4: 40% Ti) were manufactured in a vacuum carbon tube furnace by preheating from room temperature to 1700ºC (10ºC/min) and then maintaining this temperature for 1 h. Graphite crucibles were prepared to carry out the experiments. The composition of the preforms is shown in Table 2. Al ingot (5083) was placed on top of the [Ti+B_4C] preform compact to prepare the B_4C-Al composite. The crucible containing Al ingot and [Ti+B_4C] preform was placed in the furnace and heated to 1100ºC under vacuum at a rate of 10ºC/min. The peak temperature was held for 2 h, and then the crucible was cooled inside the furnace.

2.2. Phase and Microstructure Analysis

The phases of the composite materials were examined using a Philips X-ray diffraction (XRD) instrument with Cu K_α radiation at a scan rate of 10º/min. The detailed structure of the fresh interfaces was investigated by scanning electron microscopy (SEM). In addition, EDX was used to determine the composition of the phases and to analyse the matrix composite interface.

The porosity of the composite materials was measured using the Archimedes method. According to the hardness of boron carbide, the test uses the HRC hardness scale and Rockwell hardness test specification reference GB/T230-91. The fracture toughness was evaluated using a WE-10A hydraulic universal testing machine. The fracture toughness was measured by the single-edge notched beam method (specimen size = 28 mm × 4 mm × 3 mm, notch width = 0.2 mm, notch depth = 2 mm, bend span = 20 mm and load speed = 0.05 mm/min). The ASTM test standard concerning fracture toughness is ASTM E1922-04 (2010)e1.

3. Results and discussion

3.1. Phases of the Composites

The XRD patterns of the S3 [Ti+B_4C] perform with 30% Ti and the S3 B_4C-Al composite material synthesized by vacuum infiltration are shown in Fig. 1. According to the XRD results, TiB_2 was formed in the preheating treatment. As mentioned, a TiB_2 coating on the B_4C surface is desirable, as it can enhance the wettability with Al. Possible reactions (1) and (2) are thus [16]

$$5Ti+B_4C=4TiB+TiC \quad (1)$$

$$6TiB+B_4C=5TiB_2+TiC \qquad T>1300ºC \quad (2)$$

As revealed by the XRD analysis of S3 after infiltration, the Al_3BC phase existed in the composite material, which indicated that the reaction B_4C and Al occurred during the metal infiltration process. This finding confirmed that infiltration of the molten aluminium into the preform leads to reaction (3) [17]:

$$13Al_{(l)}+4B_4C_{(s)} \rightarrow 4Al_3BC_{(s)}+B(Al)+AlB_{12(s)} \ (T>985ºC) \quad (3)$$

From the XRD results, it can be seen that little Al_3BC was produced, while the AlB_{12} phase was not observed in Figure 1 due to its low content and intensity relative to the main phases.

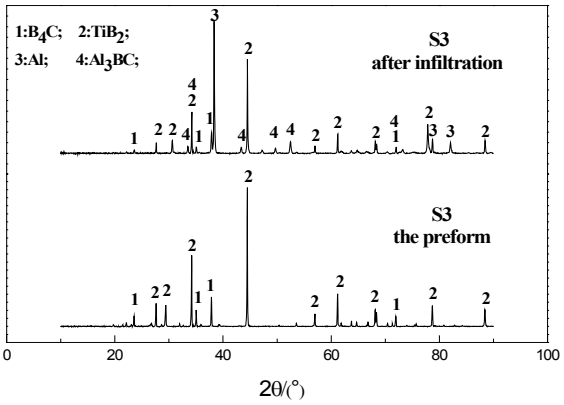

Fig. 1. XRD patterns of the S3 [Ti+B_4C] preform and S3 B_4C–Al composite material

3.2. Microstructure and Mechanical Properties

The microstructures of the [Ti+B_4C] preforms containing different Ti contents (10%, 20%, 30%, 40%) after preheating are shown in Figure 2. The microstructures observed in the images reveal that the particle size decreases and flakes appear with increasing Ti content, significantly enhancing the [Ti+B_4C] preform density. When the Ti content was 30%, the flakes were most abundant and the matrix was densest. Flakes covered almost the entire region, which exhibited a ceramic basic structure. This microstructure is consistent with the porosity test results.

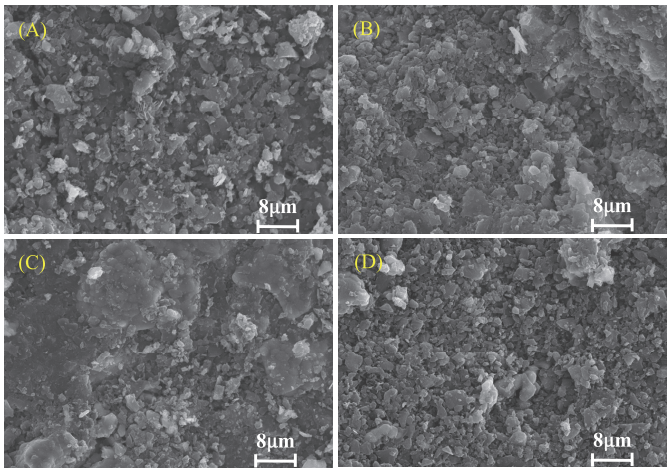

Fig. 2. SEM images of [Ti+B_4C] preforms with different Ti contents: (A) 10%, (B) 20%, (C) 30%, (D) 40%

As seen in Table 2, the porosity and hardness of composite materials have great relevance. When the Ti content is 30%, the preform porosity is 33.11% (minimum), while the corresponding composite hardness (HRC) is 63 (maximum). Figure 3 shows the hardness and porosity of the B_4C-Al composite as a function of Ti content. It can be observed that the porosity of [Ti+B_4C] perform and the hardness of B_4C-Al composite exhibit opposite behaviour with increasing Ti content. Thus, it can be concluded that the preform porosity is the factor actually affecting the hardness of B_4C-Al composite materials.

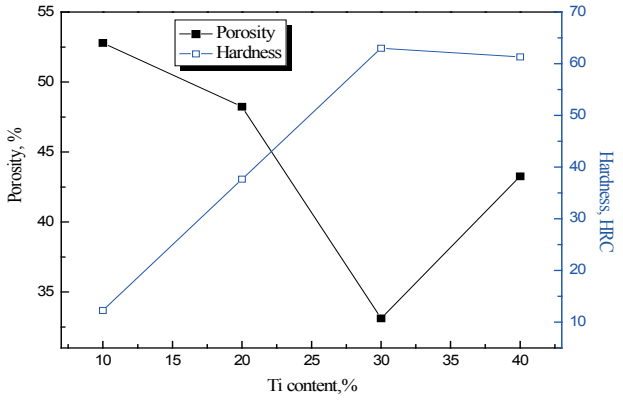

Fig. 3. Relationship between porosity and hardness

Table 2 shows the fracture toughness of B_4C-Al composite materials with various Ti contents. The trend of fracture toughness is opposite to that of the residual Al. However, the infiltration of residual Al in the preform may alter the mechanical properties of B_4C-Al composite materials. Figure 4 shows a plot of the fracture toughness and porosity of the B_4C-Al composite as a function of Ti content. It can be observed that the behaviours of the fracture toughness and porosity curves are strikingly similar. The fracture toughness of the B_4C-Al composite can also result from the residual Al content after infiltration. As the Ti content increased from 10% to 30%, both curves exhibit almost the same trend; however, as the Ti content increased from 30% to 40%, the amount of residual Al remains at approximately 10%, while the toughness increment is slight.

For the B_4C-Al composite, the aluminium content is found to be main factor affecting fracture toughness. The production of TiB_2 has in fact led to the presence of residual Al. According to the porosity results, the content of residual Al decreased with increasing Ti content, which will reduce the fracture toughness of the B_4C-Al composite.

TABLE 2

Preform properties and the mechanical properties of B_4C-Al composites

Sample	Composition	Shrinkage factor (preform)	Porosity preform (residual Al)	Hardness (HRC)	Fracture toughness (MPa·$m^{1/2}$)
S1	10% Ti, 90% B_4C	-2%	52.79%	12.25	7.75
S2	20% Ti, 80% B_4C	0.33%	48.24%	37.67	6.64
S3	30% Ti, 70% B_4C	3.3%	33.11%	63	5.03
S4	40% Ti, 60% B_4C	1%	43.26%	61.33	5.06

The preform porosity reveals that a residual amount of Al infiltrated the preforms.

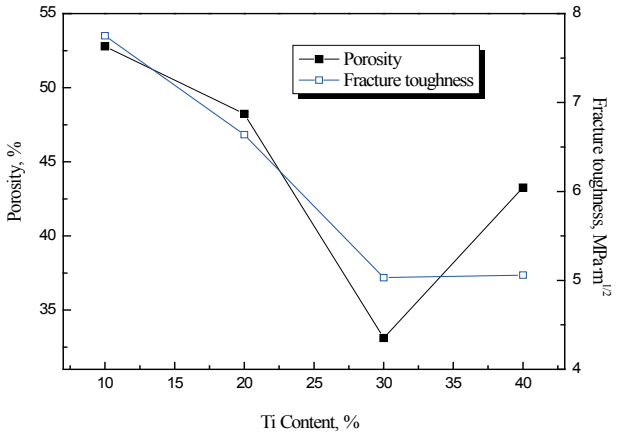

Fig. 4. Relationship between porosity and fracture toughness

Figure 5 shows the SEM images of the B_4C-Al composite materials with different Ti contents. Comparing the four micrographs, it can be observed that metal dimples exist almost everywhere in Figure 5 (A) but gradually decrease in prevalence with increasing Ti content. In addition to metal dimples, holes caused by the removal of particles were found in Figure 5 (C), whereas such holes were not clearly observed in the other micrographs. Analysing these micrographs, it can be found that the metal dimples are smaller and more fragmented in Figure 5 (C), which may be due to the compactness of the preform.

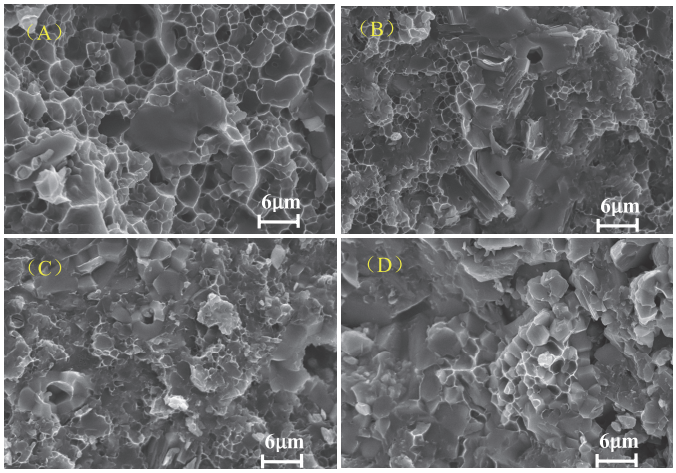

Fig. 5. SEM images of B_4C-Al composite materials with different Ti contents: (A) 10%, (B) 20%, (C) 30%, (D) 40%

The micrographs of the polished B_4C-Al composite materials with different Ti contents are shown in Figure 6. It can be observed that the silver particles gradually increased in prevalence with the Ti content and were surrounded by white rings.

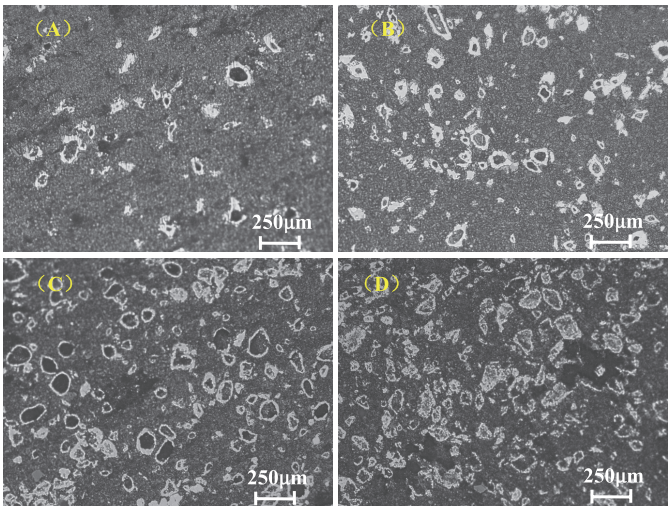

Fig. 6. Micrographs of the polished B_4C-Al composite materials with different Ti contents: (A) 10%, (B) 20%, (C) 30%, (D) 40%

To further study the main component of the B_4C-Al composite materials, the grain boundary phase analysed by EDS is shown in Figure 7. It is clear that the white rings are TiB_2, the material in the centre is Al, the outer rings of grey material are Al_3BC, and the black material is B_4C. The distribution of the materials reveals that the addition of Ti generated TiB_2, which effectively protected the existence of Al, thus avoiding the reaction of Al and B_4C. In contrast, unprotected Al participates in the interface reaction, generating a large amount of the interface product Al_3BC. These products were fabricated by these reaction formulas (1), (2) and (3) during the preheating and infiltration processes.

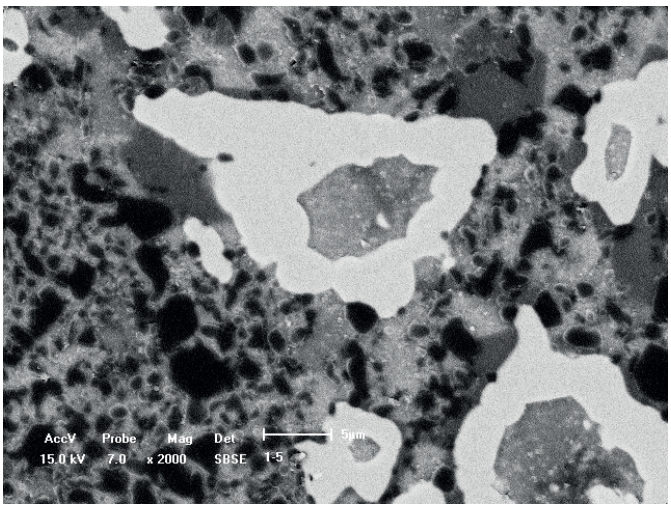

Fig. 7. SBSE image of the B_4C-Al composite materials with 20% Ti

4. Conclusion

1. In the preheating process, a TiB_2 coating formed on the B_4C surface. The XRD results for the composite material indicated the presence of the Al_3BC phase during the metal infiltration process.
2. When the Ti content is 30%, the [Ti+B_4C] preform has the minimal porosity (33.11%) and the composite has the

maximal hardness (63 HRC). The density of the preform is the factor actually affecting the hardness of the B_4C-Al composite materials.

3. The relative curves of porosity and fracture toughness are amazingly similar. The content of residual Al is found to be the main factor affecting the fracture toughness.
4. Ti addition can cause changes in the preform porosity, which triggers a series of changes in the amount of residual Al and the mechanical properties of the composites.

Acknowledgements

This work was financially supported by National Natural Science Foundation of China (No. 51204043，No. 51472048) and Major Program of the National Natural Science Foundation of China (No. 51090384).

REFERENCES

[1] X.-G. Chen, TMS, 343-350 (2006).
[2] H. Zhao, K. Hiragushi,Y. Mizota, J. Eur. Ceram. Soc**. 23**, 1485-1490 (2003).
[3] F. Tang, X. Wu, S. Ge, J. Ye, H. Zhu, M. Hagiwara, M.J. Schoenung, Wear **264**, 555-561 (2008).
[4] Q. Jiang, H. Wang, B. Ma, Y. Wang,F. Zhao, J. Alloy. Compd. **386**, 177-181 (2005).
[5] S. Yamada, K. Hirao, Y. Yamauchi, S. Kanzaki, J. Eur. Ceram. Soc. **23**, 1123-1130 (2003).
[6] H. M. Hu, E. J. Lavernia, W. C. Harrigan, J. Kajuch, S. R. Nutt, Mater. Sci. Eng. A **297,** 94-104 (2001).
[7] M. Aizenshtein, N. Froumin, N. Frage,M. P. Dariel, J. Mater. Sci. **40**, 2325-2327 (2005).
[8] J. Deng, J. Zhou, Y. Feng, Z. Ding, Ceram. Int. **28**, 425-430 (2002).
[9] S. Hayun, D. Rittel, N. Frage,M. Dariel, Mater. Sci. Eng. A **487**, 405-409 (2008).
[10] K. B. Lee, H. S. Sim, S. Y. Cho,H. Kwon, Mater. Sci. Eng. A **302**, 227-234 (2001).
[11] B.-S. Lee,S. Kang, Materials. Chem. Phys. **67**, 249–255 (2001).
[12] J. Lelito, P. Zak,J. S. Suchy, Arch. Metall. Mater. **54**, 347-350 (2009).
[13] [13]I. Dobosz, W. Gumowska, M. Uhlemann, J. Koza, Arch. Metall. Mater. **55,** 683-687 (2010).
[14] W.-F. Du, T. Watanabe, J. Eur. Ceram. Soc. **17**, 879-884 (1997).
[15] P. Lv, X. Y. Yue, L. Yu,H. Q. Ru, J. Mate.r Sc.i **44**, 3483-3487 (2009).
[16] J. Xie, S. Cao, X. Zhang, W. Li, T. Nouferr. Metal. **19**, 1468-1472 (2009).
[17] G. Arslan, F. Kara, S. Turan, Key. Eng. Mater. **264**, 1059-1062 (2004).

Received: 10 September 2014.